Polymers **2011**, *3*, 1652-1661; doi:10.3390/polym3041652

OPEN ACCESS

polymers

ISSN 2073-4360

www.mdpi.com/journal/polymers

Article

Novel Countercation in MMX-Type Mixed-Valence Chain Compound: Coexistence of Neutral and Protonated Amino Substituents

Hiroaki Iguchi [1,*], Deli Jiang [2], Jimin Xie [2], Shinya Takaishi [1] and Masahiro Yamashita [1,*]

[1] Department of Chemistry, Graduate School of Science, Tohoku University, 6-3 Aramaki-Aza-Aoba, Aoba-ku, Sendai 980-8578, Japan; E-Mail: takaishi@mail.tains.tohoku.ac.jp (S.T.)

[2] School of Chemistry and Chemical Engineering, Jiangsu University, Zhenjiang 212013, China; E-Mails: jiangdeli100@yahoo.com.cn (D.J.); xiejm@ujs.edu.cn (J.X.)

* Authors to whom correspondence should be addressed; E-Mails: h-iguchi@mail.cstm.kyushu-u.ac.jp (H.I.); yamasita@agnus.chem.tohoku.ac.jp (M.Y.); Tel.: +81-22-795-6544; Fax: +81-22-795-6548.

Received: 2 August 2011; in revised form: 7 September 2011 / Accepted: 27 September 2011 / Published: 6 October 2011

Abstract: The first MMX-type quasi-one-dimensional (Q1D) Pt chain complex (MMX chain) that contains a mono-protonated diamine as countercation, $\{o\text{-}(H_3NC_6H_4NH_2)\}_4[Pt_2(pop)_4I]\cdot H_2O$ (pop = $P_2H_2O_5^{2-}$), was synthesized. According to the crystal structural analysis, $-NH_2$ group was hydrogen-bonded to either lattice H_2O molecule or $-NH_3^+$ group in addition to typical hydrogen bond between $-NH_3^+$ group and pop ligand. To control the partial deprotonation of the countercation will be an important method for achieving the high-conductive MMX-chain polymer by the hole doping.

Keywords: MMX-chain complex; 1D structure; partial deprotonation; hydrogen bond

---

1. Introduction

Study of 1D electron system has been one of the most important subjects from the viewpoints of both fundamental and applied sciences. Conductive polymers found in the 1970s, such as polyacetylene [1,2],

have principally developed and support the current technological civilization. However, the study of conductive polymers to reveal their fundamental structure and properties has been limited because of the difficulty in making single crystals. On the other hand, conductive materials formed by the stacking of π-conjugated organic molecules were found earlier than conductive polymers [3]. The discovery of metallic behavior of TTF-TCNQ [4] attracted many scientists and promoted the studies of various Q1D charge-transfer (CT) complexes. Because these CT complexes can be obtained as single crystal, these are suitable to study the fundamentals of 1D electron system. So far, various electronic states of Q1D materials and their relationships to attractive physical properties, such as non-linearity [5,6], superconductivity [7], ferroelectricity [8] *etc.*, have been extensively studied.

Q1D halogen-bridged metal complexes have the characteristics of both conductive polymer and CT complex, that is, σ-bonded infinite chain structure and ease of making single crystal. These complexes are categorized into two groups by the number of metal ions per unit. One made from mononuclear complex (hereafter abbreviated as MX chains) has ····M─X─M─X···· infinite 1D chain structure. The other, made from lantern-type dinuclear complex (hereafter abbreviated as MMX chains) has ····M-M─X─M-M─X···· infinite 1D chain structure. MX chains has been attracting much attention because of their interesting physical properties, such as gigantic third-order nonlinear optical properties [9,10], midgap absorptions attributable to solitons and polarons [11], and charge-density-wave to Mott-Hubbard phase transition [12]. Compared with MX chains, the electrical conductivity of MMX chains is higher. To date, the measurement of electrical conductivity was performed mainly in MMX chains with dithiocarboxylate ligand, $[M_2(RCS_2)_4I]$ (M = Ni, Pt; R = alkyl chain group) [13-17]. It was reported that $Pt_2(CH_3CS_2)_4I$ showed high conductivity, 13 S cm^{-1}, at room temperature, and metal-insulator transition at 300 K [14]. On the other hand, MMX chains with pop ligand, $A_4[Pt_2(pop)_4X]\cdot nH_2O$ (A = Li, K, Cs, NH_4 *etc.*; X = Cl, Br, I) [18-20], have lower conductivity [14]. However, pop-type MMX chains are more attractive because it is easier to synthesize various derivatives by changing countercations. Moreover, the new electronic state [21], photo-induced phase transition [22] and vapor-induced reversible switching of the electronic state and the electrical conductivity [23-26] have been reported, recently.

In order to achieve the higher electrical conductivity in pop-type MMX chains, the doping of hole or electron into 1D chain is a promising method, though no trials have succeeded. Herein, we report the first MMX chains containing mono-protonated diamine as countercation, $\{o\text{-}(H_3NC_6H_4NH_2)\}_4[Pt_2(pop)_4I]\cdot H_2O$ (**1**), which can be the clue to the doping.

2. Experimental Section

2.1. Materials

All commercially available chemicals are of reagent grade and used as received without further purification. The starting $Pt(II)_2$ and $Pt(III)_2$ dinuclear complexes, $K_4[Pt_2(pop)_4]\cdot 2H_2O$ and $K_4[Pt_2(pop)_4I_2]$, respectively, were synthesized from K_2PtCl_4, H_3PO_3, and I_2 according to literature method [27,28]. $\{o\text{-}(H_3NC_6H_4NH_3)\}SO_4$ was synthesized as follows: $o\text{-}(H_2NC_6H_4NH_2)$ was dissolved in ethanol and added equimolar conc. H_2SO_4. Resulting white solid was filtered and dried in vacuum to afford $\{o\text{-}(H_3NC_6H_4NH_3)\}SO_4$.

*2.2. Synthesis of {o-($H_3NC_6H_4NH_2$)}$_4$[Pt_2(pop)$_4$I]·H_2O (**1**)*

$K_4[Pt_2(pop)_4]\cdot 2H_2O$ (29.9 mg, 0.026 mmol) and $K_4[Pt_2(pop)_4I_2]$ (30.5 mg, 0.022 mmol) were dissolved in water (4 mL). 200 mM {*o*-($H_3NC_6H_4NH_3$)}SO_4 aqueous solution was also prepared. Single crystals of **1** suitable for X-ray crystal structural analysis were grown by the standard diffusion method using glass cell. 1 mL of 200 mM {*o*-($H_3NC_6H_4NH_3$)}SO_4 aqueous solution was loaded at the end of the cell, then 1 mL of the Pt complex solution was carefully loaded above and allowed to stand for a few days. Brown needle-like crystals of **1** were obtained in 44% yield with the red crystalline by-products, $Pt(III)_2$ dinuclear complex, in 4% yield. Further standing of the solution caused a redissolution of the crystals of **1** and an increase of the amount of by-products.

2.3. X-Ray Single Crystal Structural Analysis

The X-ray diffraction experiments for **1** were carried out on a Bruker SMART CCD diffractometer with graphite-monochromated Mo-Kα radiation (λ = 0.71073 Å). The crystal structures were solved by the directed method followed by Fourier syntheses. Structure refinement was performed by full matrix least-squares procedures using SHELXL-97 on F^2 [29]. Hydrogen atoms binding to aromatic ring were treated with a riding model, though those binding to nitrogen or oxygen atoms were not refined because of low reliability especially for **1**, which contains heavy atoms. Crystallographic data and structural refinement parameters for **1** are summarized in Table 1.

Table 1. Crystallographic data and structural refinement parameters for **1**.

Empirical formula	$C_{24}H_{46}IN_8O_{21}P_8Pt_2$
Formula weight	1,547.53
Crystal size (mm)	0.22 × 0.02 × 0.005
Temperature (K)	150(2)
Crystal system	Triclinic
Space group	*P*-1
a (Å)	8.943(2)
b (Å)	11.788(3)
c (Å)	12.242(3)
α (°)	110.610(5)
β (°)	104.207(6)
γ (°)	96.077(6)
Volume (Å^3)	1144.5(5)
Z	1
D(calc.) (g cm^{-3})	2.245
μ(Mo-Kα) (mm^{-1})	7.143
F(000)	743
Theta range (−)	1.87–30.05
Total reflections	11588
Unique reflections	6419
Goodness of fit	0.914
R, wR_2 [$I > 2\sigma(I)$]	0.0525, 0.0915
R, wR_2 (all data)	0.0846, 0.1021

Crystallographic data for **1** have been deposited with the Cambridge Crystallographic Data Center as supplementary publication No. CCDC-836700. These data can be obtained free of charge from the Cambridge Crystallographic Data Centre via www.ccdc.cam.ac.uk/data_request/cif.

3. Results and Discussion

ORTEP representation of the molecular structure of **1** at 150 K is shown in Figure 1. Except half of the $[Pt_2(pop)_4]I$ chain unit generated by symmetry operation, labeled atoms belong to the asymmetric unit. Since bridging I^- ion (I1) is disordered and lattice water molecule (O11) was at the inversion center, the occupancy of I1 and O11 is 50%. Although relatively large thermal ellipsoids observed in N3, N4 and C9 to C12 may suggest the disorder of the molecule, neither the trial to separate the two components nor that to select lower symmetric space group (*P*1) provided appropriate thermal factors.

Figure 1. ORTEP representation of the molecular structure of **1**. Thermal ellipsoids are displayed at the 50% probability level. Hydrogen atoms are omitted for clarity. The occupancy of I1 and O11 are 50%. Symmetry transformations used to generate equivalent atoms: #1: $-x, -y + 1, -z$.

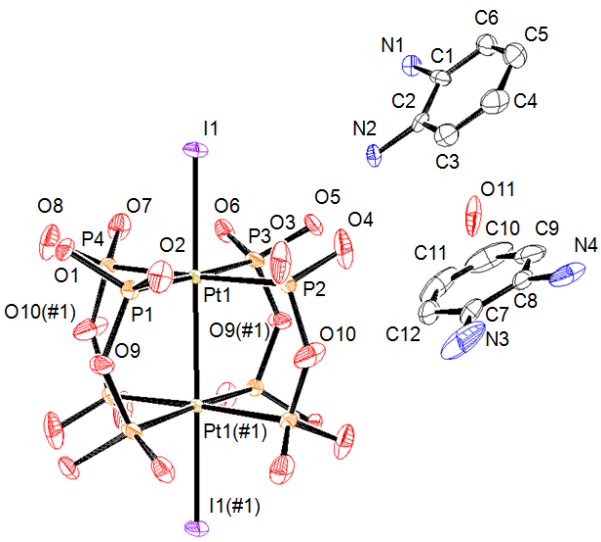

Figure 2 shows the crystal structure of **1** with the representation of the unit cell. Two neighboring $[Pt_2(pop)_4]$ units are bridged by an I^- ion, forming a ···Pt–Pt–I–Pt–Pt–I··· linear-chain structure along the *a*-axis. The bridging I^- ions are disordered with half occupancies at displaced position from the midpoints between the neighboring two $[Pt_2(pop)_4]$ units. As shown in Table 2, Pt-Pt distance (*d*(Pt-Pt) = 2.8470(10) Å) is almost intermediate value of that of $Pt(II)_2$ dinuclear complex, $K_4[Pt_2(pop)_4]\cdot 2H_2O$, (*d*(Pt-Pt) = 2.925(1) Å) [18], and that of $Pt(III)_2$ dinuclear complex, $K_4[Pt_2(pop)_4I_2]$, (*d*(Pt-Pt) = 2.754(1) Å) [30]. This indicates that **1** is Pt(II)-Pt(III) mixed-valence compound [18,20,31].

Figure 2. Crystal structure of **1** viewed along **(a)** *a*-axis and **(b)** *b*-axis. Hydrogen atoms are omitted for clarity. Unit cell is described as blue dashed line. (black, C; blue, N; red, O; orange, P; purple, I; yellow, Pt).

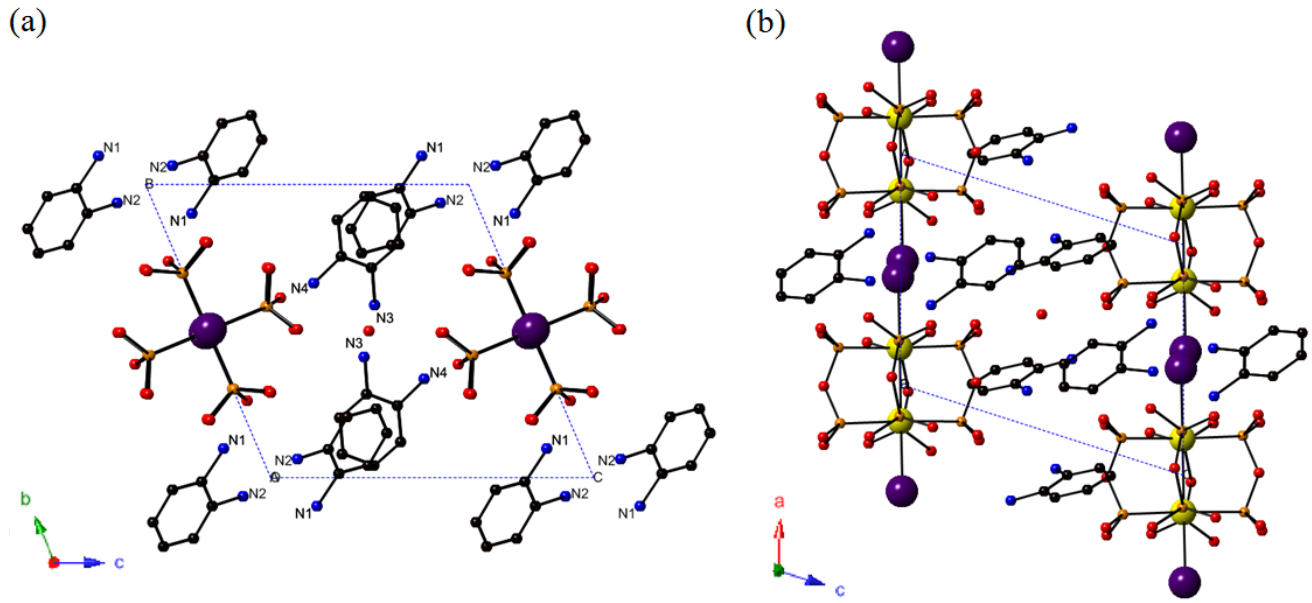

Table 2. Selected bond length (Å) and angles (°) for **1**.

Pt(1)-Pt(1)#1	2.8470(10)	Pt(1)-I(1)-I(1)#2	161.9(3)
Pt(1)-I(1)	2.7341(14)		
Pt(1)-I(1)#2	3.3660(13)		

Symmetry transformations used to generate equivalent atoms: #1: $-x, -y + 1, -z$; #2: $-x + 1, -y + 1, -z$.

Interestingly, one $[Pt_2(pop)_4]$ unit, one bridging I^- ion and four *o*-phenylenediamine molecules as countercations exist in a unit cell. Because the charge of the chain unit (···$[Pt_2(pop)_4]I$···) is −4, *o*-phenylenediamine molecules should be monocation, *o*-$(H_3NC_6H_4NH_2)^+$, not dication, *o*-$(H_3NC_6H_4NH_3)^{2+}$, that we have expected. This partial deprotonation of diammonium ion has not been observed in any MMX chains synthesized so far. Although several kinds of compounds containing mono-protonated diamines as countercation have been reported [32-36], these compounds were synthesized from neutral diamines with acid. It should be noted that **1** differs from them in that it was synthesized from fully protonated diammonium, {*o*-$(H_3NC_6H_4NH_3)$}SO_4, via the deprotonation. To our knowledge, only the organic-inorganic hybrid compounds, $(NH_3\text{-}R\text{-}NH_3)(NH_3\text{-}R\text{-}NH_2)PbI_5$ (R = 5,5'-bis(ethylsulfanyl)-2,2'-bithiophene) [37], is the other example which was synthesized through similar mechanism and whose structure was well-defined by the X-ray single crystal structural analysis.

In order to reveal the detail of the partial deprotonation, we focused on the assignment of $–NH_2$ and $–NH_3^+$ group. It has been known that the chain structure of MMX chains with pop ligands is stabilized by the hydrogen bonds between alkyl ammonium ions (RNH_3^+) and oxygen atoms of pop ligands (–P=O···H-N^+-H···O=P–). Consequently, the nitrogen atom which is close to oxygen atoms in both $[Pt_2(pop)_4]$ units belongs to -NH_3^+ group. As shown in Table 3, N1 and N4 are close (d(N···O) < 3.0 Å) to two or more oxygen atoms in pop ligands (O2 and O6 for N1, O3, O4 and O7 for N4). Therefore, N1 and N4 belong to -NH_3^+ group, and N2 and N3 belong to $–NH_2$ group.

Table 3. Selected interatomic distance (Å) for **1**. The distances shorter than 3.0 Å are represented in bold font.

N(1)-O(2)#3	**2.778(9)**	N(3)-O(4)	3.438(13)
N(1)-O(6)#4	**2.793(9)**	N(3)-O(8)#1	3.405(15)
N(1)-N(2)#4	**2.858(10)**	N(3)-O(11)	3.031(12)
N(2)-O(1)#2	3.987(9)	**N(4)-O(3)#5**	**2.870(13)**
N(2)-O(5)	3.026(9)	**N(4)-O(4)#5**	**2.926(11)**
		N(4)-O(7)#6	**2.966(12)**
		N(4)-O(8)#6	3.074(12)
		N(4)-O(11)	3.065(13)

Symmetry transformations used to generate equivalent atoms: #1: $-x, -y + 1, -z$; #2: $-x + 1, -y + 1, -z$; #3: $x, y - 1, z$; #4: $-x + 1, -y, -z$; #5: $-x + 1, -y + 1, -z + 1$; #6: $x, y, z + 1$.

Figure 3. Crystal structure of **1** focusing on the *o*-$(H_3NC_6H_4NH_2)^+$ ion pairs. Hydrogen atoms are omitted for clarity. Short contacts are indicated by gray dashed lines. (black, C; blue, N) **(a)** *o*-$(H_3N(1)C_6H_4N(2)H_2)^+$ ions. **(b)** *o*-$(H_3N(4)C_6H_4N(3)H_2)^+$ ions and lattice water molecules.

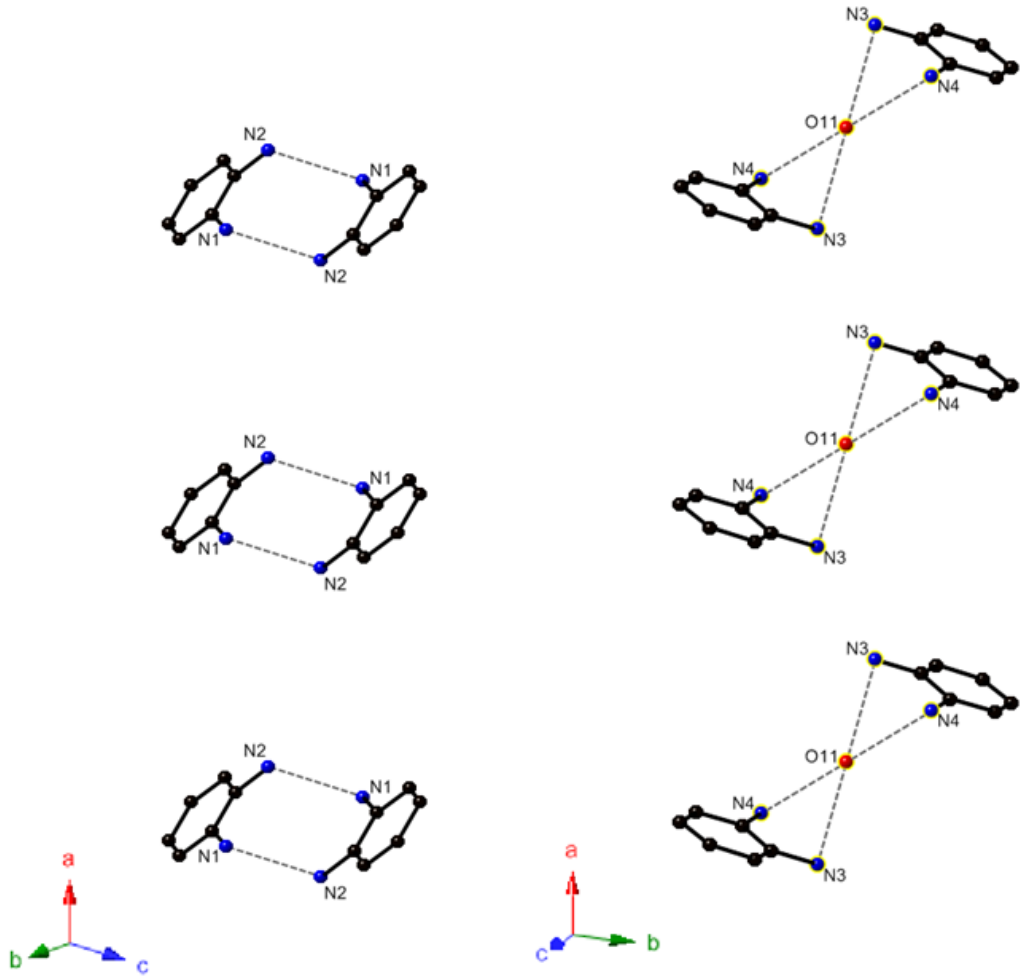

(a) **(b)**

In addition, the short intermolecular N1–N2 distance (2.858(10) Å) suggests the existence of hydrogen bond between $-NH_2$ and $-NH_3^+$ group. Focusing on the *o*-$(H_3N(1)C_6H_4N(2)H_2)^+$ molecules, this N-H···N hydrogen bond induces the pairing of neighbor two molecules as shown in Figure 3(a). In case of *o*-$(H_3N(4)C_6H_4N(3)H_2)^+$ molecules, relatively short N-O distances, *d*(N3-O11) = 3.031(12) Å and *d*(N4-O11) = 3.065(13) Å, suggest the existence of some interactions between these molecules and lattice water molecules. Although the position of the hydrogen atoms are unclear, N-H···O and N···H-O hydrogen bonds are possibly the origin of these interactions. As shown in Figure 3(b), a *o*-$(H_3N(4)C_6H_4N(3)H_2)^+$ molecule is paired with another one via a lattice water molecule.

The most promising property expected from partial deprotonation is the hole doping of the semiconducting chain. Very recently, the hole doping by the deprotonation of counteranion was achieved in a conducting CT complex [38], thus this method can be effective for MMX chains. However, **1** is still in closed-shell system because total positive charge of countercation is +4 per formula. In order to achieve the hole doping and high conductivity, it is necessary to decrease the total positive charge to non-integral value with keeping four *o*-phenylenediamine molecules in a formula. Since fully protonated *o*-$(H_3NC_6H_4NH_3)^{2+}$ ion, mono-protonated *o*-$(H_3NC_6H_4NH_2)^+$ ion and neutral *o*-$(H_2NC_6H_4NH_2)$ molecule are held in equilibrium in aqueous solution, the tuning of synthetic condition such as pH and concentration may provide the desired material. These further works are currently in progress.

4. Conclusions

$\{o\text{-}(H_3NC_6H_4NH_2)\}_4[Pt_2(pop)_4I]\cdot H_2O$ (**1**) was synthesized as the first MMX chain containing partially deprotonated countercation. The crystal structure of **1** was solved by the X-ray single crystal structural analysis. Since four *o*-phenylenediamine molecules exist in a formula, half of nitrogen atoms were expected to be deprotonated. A close examination of the structure confirmed this expectation. N1 and N4 were protonated nitrogen supporting 1D chain structure by hydrogen bond to pop ligands. On the other hand, N2 and N3 were neutral nitrogen forming hydrogen bond with $-NH_3^+$ group and lattice water molecules, respectively.

Further tuning of the synthetic condition of **1** will develop an effective method for partial deprotonation, which is one of the keys to achieve hole doping, inducing high conductivity of MMX chains.

Acknowledgments

This work was partly supported by the Grant-in-Aid for Creative Scientific Research from the Ministry of Education, Culture, Sports, Science and Technology, by the Global COE Program at Tohoku University and by the Tohoku University Institute for International Advanced Research and Education.

References

1. Shirakawa, H.; Louis, E.J.; MacDiarmid, A.G.; Chiang, C.K.; Heeger, A.J. Synthesis of electrically conducting organic polymers: Halogen derivatives of polyacetylene, $(CH)_x$. *J. Chem. Soc. Chem. Commun.* **1977**, 578-580.

2. Chiang, C.K.; Fincher, C.R.; Park, Y.W.; Heeger, A.J.; Shirakawa, H.; Louis, E.J.; Gau, S.C.; MacDiarmid, A.G. Electrical conductivity in doped polyacetylene. *Phys. Rev. Lett.* **1977**, *39*, 1098-1101.
3. Akamatu, H.; Inokuchi, H.; Matsunaga, Y. Electrical conductivity of the perylene-bromine complex. *Nature* **1954**, *173*, 168-169.
4. Ferraris, J.P.; Cowan, D.O.; Walatka, V.V.; Perlstein, J.H. Electron transfer in a new highly conducting donor-acceptor complex. *J. Am. Chem. Soc.* **1973**, *95*, 948-949.
5. Tokura, Y.; Okamoto, H.; Koda, T.; Mitani, T.; Saito, G. Nonlinear electric transport and switching phenomenon in the mixed-stack charge-transfer crystal tetrathiafulvalene-*p*-chloranil. *Phys. Rev. B* **1988**, *38*, 2215-2218.
6. Kriza, G.; Quirion, G.; Traetteberg, O.; Kang, W.; Jérome, D. Shapiro interference in a spin-density-wave system. *Phys. Rev. Lett.* **1991**, *66*, 1922-1925.
7. Saito, G.; Yoshida, Y. Organic superconductors. *Chem. Rec.* **2011**, *11*, 124-145.
8. Horiuchi, S.; Kumai, R.; Okimoto, Y.; Tokura, Y. Chemical approach to neutral-ionic valence instability, quantum phase transition, and relaxor ferroelectricity in organic charge-transfer complexes. *Chem. Phys.* **2006**, *325*, 78-91.
9. Kishida, H.; Matsuzaki, H.; Okamoto, H.; Manabe, T.; Yamashita, M.; Taguchi, Y.; Tokura, Y. Gigantic optical nonlinearity in one-dimensional Mott-Hubbard insulators. *Nature* **2000**, *405*, 929-932.
10. Tao, S.; Miyagoe, T.; Maeda, A.; Matsuzaki, H.; Ohtsu, H.; Hasegawa, M.; Takaishi, S.; Yamashita, M.; Okamoto, H. Ultrafast optical switching by using nanocrystals of a halogen-bridged nickel-chain compound dispersed in an optical polymer. *Adv. Mater.* **2007**, *19*, 2707-2710.
11. Okamoto, H.; Yamashita, M. Solitons, polarons, and excitons in quasi-one-dimensional halogen-bridged transition metal compounds. *Bull. Chem. Soc. Jpn.* **1998**, *71*, 2023-2039.
12. Takaishi, S.; Takamura, M.; Kajiwara, T.; Miyasaka, H.; Yamashita, M.; Iwata, M.; Matsuzaki, H.; Okamoto, H.; Tanaka, H.; Kuroda, S.; Nishikawa, H.; Oshio, H.; Kato, K.; Takata, M. Charge-density-wave to mott-hubbard phase transition in quasi-one-dimensional bromo-bridged Pd compounds. *J. Am. Chem. Soc.* **2008**, *130*, 12080-12084.
13. Bellitto, C.; Flamini, A.; Gastaldi, L.; Scaramuzza, L. Halogen oxidation of tetrakis(dithioacetato)diplatinum(II) complexes, $Pt_2(CH_3CS_2)_4$. Synthesis and characterization of $Pt_2(CH_3CS_2)_4X_2$ (X = Cl,Br,I) and Structural, electrical, and optical properties of linear-chain (μ-Iodo)tetrakis(dithioacetato)diplatinum, $Pt_2(CH_3CS_2)_4I$. *Inorg. Chem.* **1983**, *22*, 444-449.
14. Kitagawa, H.; Onodera, N.; Sonoyama, T.; Yamamoto, M.; Fukawa, T.; Mitani, T.; Seto, M.; Maeda, Y. Charge ordering with lattice distortions in a conductive MMX-chain complex, $Pt_2(dta)_4I$ (*dta* = $CH_3CS_2^-$). *J. Am. Chem. Soc.* **1999**, *121*, 10068-10080.
15. Mitsumi, M.; Murase, T.; Kishida, H.; Yoshinari, T.; Ozawa, Y.; Toriumi, K.; Sonoyama, T.; Kitagawa, H.; Mitani, T. Metallic behavior and periodical valence ordering in a MMX chain compound, $Pt_2(EtCS_2)_4I$. *J. Am. Chem. Soc.* **2001**, *123*, 11179-11192.
16. Mitsumi, M.; Yoshida, Y.; Kohyama, A.; Kitagawa, Y.; Ozawa, Y.; Kobayashi, M.; Toriumi, K.; Tadokoro, M.; Ikeda, N.; Okumura, M.; Kurmoo, M. Syntheses, structures and solid-state properties of MMX mixed-valence chains, $[Ni^{II/III}_2(RCS_2)_4I]_\infty$ (R = Et, *n*-Pr and *n*-Bu): Evidence of a spin-peierls transition. *Inorg. Chem.* **2009**, *48*, 6680-6691.

17. Mitsumi, M.; Yamashita, T; Aiga, Y; Toriumi, K; Kitagawa, H; Mitani, T; Kurmoo, M. On the nature of the multiple ground states of the MMX mixed-valence chain compound, $[Pt^{II/III}_2(n\text{-PenCS}_2)_4I]_\infty$. *Inorg. Chem.* **2011**, *50*, 4368-4377.
18. Che, C.-M.; Herbstein, F.H.; Schaefer, W.P.; Marsh, R.E.; Gray, H.B. Binuclear platinum diphosphite complexes. Crystal structures of $K_4[Pt_2(pop)_4Br]\cdot 3H_2O$, a new linear chain semiconductor, and $K_4[Pt_2(pop)_4Cl_2]\cdot 2H_2O$. *J. Am. Chem. Soc.* **1983**, *105*, 4604-4607.
19. Kurmoo, M.; Clark, R.J.H. Spectroscopic studies on linear-chain semiconductors and related species. Vibrational and resonance raman spectroscopy of the diphosphite complexes $K_4[Pt_2(pop)_4]\cdot 2H_2O$, $K_4[Pt_2(pop)_4X_2]\cdot 2H_2O$, and $K_4[Pt_2(pop)_4X]\cdot nH_2O$, X = Cl, Br, I. *Inorg. Chem.* **1985**, *24*, 4420-4425.
20. Clark, R.J.H.; Kurmoo, M.; Dawes, H.M.; Hursthouse, M.B. Binuclear platinum diphosphite complexes: X-ray crystal structures of $K_4[Pt_2(pop)_4Cl]\cdot 3H_2O$ and $K_4[Pt_2(pop)_4Br_2]\cdot 2H_2O$ (pop = $P_2O_5H_2^{2-}$). *Inorg. Chem.* **1986**, *25*, 409-412.
21. Iguchi, H.; Takaishi, S.; Kajiwara, T.; Miyasaka, H.; Yamashita, M.; Matsuzaki, H.; Okamoto, H. Mixed charge-ordering state of MMX-Type quasi-one-dimensional iodide-bridged platinum complexes with binary countercations. *J. Am. Chem. Soc.* **2008**, *130*, 17668-17669.
22. Matsuzaki, H.; Matsuoka, T.; Kishida, H.; Takizawa, K.; Miyasaka, H.; Sugiura, K.; Yamashita, M.; Okamoto, H. Novel Optical and magnetic bistability and photoinduced transition in a one-dimensional halogen-bridged binuclear Pt complex. *Phys. Rev. Lett.* **2003**, *90*, 046401:1-046401:4.
23. Matsuzaki, H.; Kishida, H.; Okamoto, H.; Takizawa, K.; Matsunaga, S.; Takaishi, S.; Miyasaka, H.; Sugiura, K.; Yamashita, M. Vapochromic behavior accompanied by phase transition between charge-polarization and charge-density-wave states in a quasi-one-dimensional iodine-bridged dinuclear platinum compound. *Angew. Chem. Int. Ed.* **2005**, *44*, 3240-3243.
24. Yamashita, M.; Takizawa, K.; Matsunaga, S.; Kawakami, D.; Iguchi, H.; Takaishi, S.; Kajiwara, T.; Iwahori, F.; Ishii, T.; Miyasaka, H.; Sugiura, K.; Matsuzaki, H.; Kishida, H.; Okamoto, H. Versatile vapochromic behavior accompanied by a phase change between charge-polarization state and charge-density-wave state in a quasi-one-dimensional iodo-bridged dinuclear platinum mixed-valence compound, $[\{NH_3(CH_2)_5NH_3\}_2][Pt_2(pop)_4I]\cdot 4H_2O$. *Bull. Chem. Soc. Jpn.* **2006**, *79*, 1404-1406.
25. Iguchi, H.; Takaishi, S.; Kajiwara, T.; Miyasaka, H.; Yamashita, M.; Matsuzaki, H.; Okamoto, H. Direct synthesis and crystal structure of dehydrated state in vapochromic MMX-type quasi-one-dimensional iodide-bridged platinum complexes. *J. Inorg. Organomet. Polym. Mater.* **2009**, *19*, 85-90.
26. Iguchi, H.; Takaishi, S.; Miyasaka, H.; Yamashita, M.; Matsuzaki, H.; Okamoto, H.; Tanaka, H.; Kuroda, S. Water-vapor-induced reversible switching of electronic states in a MMX-type chain complex with retention of single crystallinity. *Angew. Chem. Int. Ed.* **2010**, *49*, 552-555.
27. Che, C.-M.; Butler, L.G.; Gray, H.B. Spectroscopic properties and redox chemistry of the phosphorescent excited state of $Pt_2(P_2O_5)_4H_8^{4-}$. *J. Am. Chem. Soc.* **1981**, *103*, 7796-7797.
28. Kimura, N.; Ohki, H.; Ikeda, R.; Yamashita, M. Valence structure of one-dimensional halogen bridged -Pt-Pt-X-Pt-Pt-X- type complexes studied by ^{31}P solid NMR. *Chem. Phys. Lett.* **1994**, *220*, 40-45.

29. Sheldrick, G.M. *SHSLXL97*, *Program for Crystal Structure Refinement*; University of Göttingen: Göttingen, Germany, 1997.
30. Alexander, K.A.; Bryan, S.A.; Fronczek, F.R.; Fultz, W.C.; Rheingold, A.L.; Roundhill, D.M.; Stein, P.; Watkins, S.F. Crystal and molecular structures of dihalotetrakis(pyrophosphito)diplatinum(III) complexes. Integrative use of structural and vibrational data to assess intermetallic bonding and the trans influence of the Pt(III)-Pt(III) bond. *Inorg. Chem.* **1985**, *24*, 2803-2808.
31. Takizawa, K.; Ishii, T.; Miyasaka, H.; Matsuzaka, H.; Yamashita, M.; Kawashima, T.; Matsuzaki, H.; Kishida, H.; Okamoto, H. Crystal and electronic structures of quasi-one-dimensional halogen-bridged binuclear platinum complexes, $\{(C_nH_{2n+1})_2NH_2\}_4[Pt_2(pop)_4I]$ (n = 2–6). *Mol. Cryst. Liq. Cryst.* **2002**, *376*, 159-164.
32. Shi, S.; Wang, L.; Yuan, H.; Li, G.; Xu, J.; Zhu, G.; Song, T. Qiu, S. Hydrothermal synthesis and characterization of a new 3D vanadium(III) phosphate $(C_4H_8N_2H_4)_{0.5}(C_4H_8N_2H_3)[V_4(HPO_3)_7(H_2O)_3]1.5H_2O$. *J. Solid State Chem.* **2004**, *177*, 4183-4187.
33. Arumuganathan, T.; Rao, A.S.; Das, S.K. Non-covalent O···O interactions among isopolyanions using a cis-$\{MoO_2\}$ moiety by the assistance of N–H···O hydrogen bonds. *J. Chem. Sci.* **2008**, *120*, 297-304.
34. Wang, J.; Fan, J.; Zhang, W.-G.; Wang, Z.-H.; Tan, J.-B. Synthesis and crystal structure of a new binuclear samarium complex with salicylate. *J. Chem. Crystallogr.* **2009**, *39*, 585-588.
35. Chatterjee, T.; Sarma, M.; Das, S.K. Polyoxometalate associated ion-pair solid based on a crown ether inclusion complex: Synthesis, structure and spectroscopy. *J. Mol. Struct.* **2010**, *981*, 34-39.
36. Guo, H.-X.; Li, X.-Z.; Weng, W. Hydrothermal synthesis, crystal structure and electrochemical property of a novel 3-D microporous reduced molybdophosphate with large cavities. *Inorg. Chem. Commun.* **2010**, *13*, 909-913.
37. Zhu, X.-H.; Mercier, N.; Allain, M.; Frère, P.; Blanchard, P.; Roncali, J.; Riou, A. Crystal structure of $(NH_3–R–NH_3)(NH_3–R–NH_2)PbI_5$ (*R*=5,5'-bis(ethylsulfanyl)-2,2'-bithiophene): $NH_3^+…NH_2$ interaction as a tool to reach densely packed organic layers in organic-inorganic perovskites. *J. Solid State Chem.* **2004**, *177*, 1067-1071.
38. Lakhdar, Y.; Mézière, C.; Zorina, L.; Giffard, M.; Batail, P.; Canadell, E.; Auban-Senzier, P.; Pasquier, C.; Jérome, D.; Náfrádi, B.; Fórró, L. Dual [proton]/[hole] mixed valence in a molecular metal: Balancing chemical activity in the solid state by tapping into a molecular hole reservoir. *J. Mater. Chem.* **2011**, *21*, 1516-1522.